Fast T_1 Mapping of Mouse Brain at 7 T with Time-optimized Partial Inversion Recovery utilizing a Surface Coil

N. Kobayashi[1], H. Igarashi[1], and T. Nakada[1]

[1]Center for Integrated Human Brain Science, Brain Research Institute, University of Niigata, Niigata, Japan

Introduction

Measurement of the longitudinal relaxation time constant, T_1, with inversion recovery sequence (IR) is a time consuming process, because the recovery delay prior to spin inversion must be sufficiently long to allow magnetization to relax toward equilibrium. Additionally, spatial variation of radiofrequency (RF) field induces heterogenous efficiency of spin inversion, leading to significant errors on T_1 quantification, especially when using a surface coil for RF transmission. Here, we present a novel fast T_1 mapping method utilizing a surface coil, called Time–Optimized Partial Inversion Recovery (TOPIR). The method employs a spin preparation module for T_1 mapping with partial inversion recovery (TAPIR), in which a saturation pulse followed by a delay, τ, is introduced before each inversion for avoiding the full recovery requirement (1). Imperfection of spin inversion and saturation due to the inhomogenous RF field, which is a deleterious error source on accurate T_1 estimation (2), was compensated by employing adiabatic pulses: HS1 for inversion (3) and BIR–4 for saturation (4).

Theory

The concept of the time–optimization is to minimize the total scan time under the condition that dynamic range of the sampled relaxation curve is sufficiently wide for spins with T_1 comparable to or shorter than a reference longitudinal relaxation time T_1^{ref}. In the case of partial inversion recovery, if the first point is sampled immediately after the spin inversion, dynamic range of the recovery curve, $2M_0\varepsilon$, is determined depending on the delay τ between saturation and inversion, and the longest inversion time TI^{max} (Fig.1). In this study, TIs were set as a geometrical series with a common ratio of 2. The optimal values of τ and TI^{max} are obtained for a designated normalized dynamic range of ε ($0 \le \varepsilon \le 1$) by analytically minimizing the total scan time (Fig.2):

$$\tau = -T_1^{ref} \log\left\{\frac{(2-\varepsilon)n_{TI} + 2\varepsilon - \sqrt{\varepsilon^2 n_{TI}^2 + 4\varepsilon(2-\varepsilon) + 4\varepsilon^2}}{n_{TI}}\right\}, \qquad TI^{max} = T_1^{ref} \log\left\{\frac{2-\exp(-\tau/T_1^{ref})}{2(1-\varepsilon)-\exp(-\tau/T_1^{ref})}\right\}$$

Methods

All MRI experiments were performed in a horizontal 7T magnet using a surface coil with a diameter of 2 cm for RF transmission and signal reception. The time–optimization parameters of T_1^{ref} = 1800 ms, n_{TI} = 6, ε = 0.7–0.9 were employed, resulting in a total scan time of 20–36 sec (Fig.2). In this sequence, after each TOPIR spin preparation, a single snapshot–FLASH with the centric–out k–space filling was performed to acquire the recovering longitudinal magnetization (5). Sequence parameters of the snapshot–FLASH module were as follows: TR/TE = 4.8/2.4 ms, matrix size = 96×96, FOV = 15.4×15.4 mm^2, and slice thickness = 2 mm. Relatively high excitation flip angles, FA = 20–40°, were employed to ensure sufficient SNR. Conventional IR measurement (cIR), $\varepsilon \cong 1$, was performed for comparison. First, the method was validated by measuring phantoms filled with different concentrations of Gd–DTPA solution; $T_1 \cong$ 900–3200 ms. Second, T_1 maps of male C57BL mouse at the age of ~10 weeks (n = 5) were acquired, and the T_1 estimates were compared between the optimization conditions for three anatomical regions.

Results and Discussion

Phantom measurement showed comparable T_1 estimates regardless of dynamic range of the sampled recovery curve; the difference fell within 4% over the T_1 range of 900–3200 ms. T_1 maps of a mouse brain represented consistent T_1 values in the majority of brain tissues (Fig.3). There were regions with relatively high T_1 values found on the map from cIR in the vicinity of internal carotid and middle cerebral arteries due to an influx of brood (arrow), whereas those were not detected on the maps with TOPIR. On TOPIR, the effect of longitudinal relaxation caused by spins outside the RF field flowing into the imaging slice is reduced by minimizing the duration of the spin preparation module. Cerebral spinal fluid (CSF) showed a decreasing trend of T_1 as the dynamic range was squeezed (arrow head). Tissues with longitudinal relaxation times ≤ T_1^{ref} (1800 ms) were sampled with relatively wide dynamic range, and thus yielded accurate T_1, whereas spins with T_1 much larger than T_1^{ref}, such as CSF, suffered from underestimation. The T_1 values of the three anatomical areas were comparable regardless of dynamic range and FA (Table 1). The train of successive excitation pulses in snapshot–FLASH module modulates the recovery process depending on the flip angle (1). Although the considerable spatial variation of the RF field due to excitation with the surface coil can induce errors, the centric–out k–space filling minimized the effects, and therefore dependence on the excitation flip angle was negligible. Overall, the current method can conquer the difficulties of T_1 quantification with a surface coil for RF transmission.

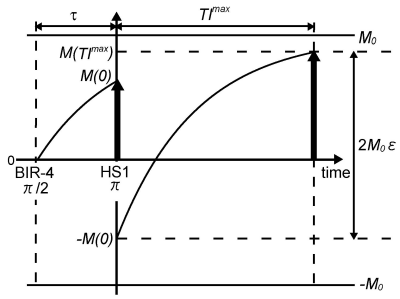

Fig.1 Paradigm of the relaxation process on partial inversion recovery.

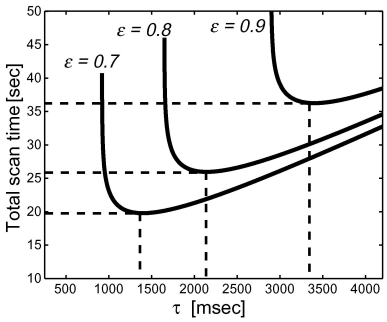

Fig.2 Optimal delay τ and the minimal total scan time are obtained at the minimum point.

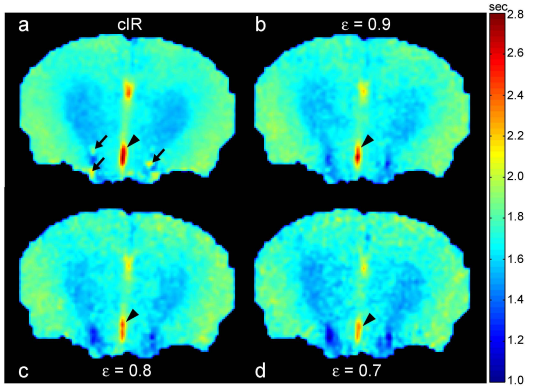

Fig.3 T_1 maps of mouse brain measured by cIR and TOPIR with ε=0.7–0.9.

Table 1. Comparison of estimated T_1 values measured by TOPIR and cIR sequence. T_1 values of three ROIs are shown along with the standard deviation (n = 5). [a] CC, cerebral cortex; [b] HC, hippocampus; [c] BG, basal ganglia.

	FA=20°			FA=30°			FA=40°		
	CC[a]	HC[b]	BG[c]	CC[a]	HC[b]	BG[c]	CC[a]	HC[b]	BG[c]
cIR	1831±26	1782±29	1612±23	1813±21	1757±31	1602±10	1820±24	1762±34	1613±9
ε=0.9	1853±36	1790±39	1631±13	1847±37	1776±34	1634±9	1847±44	1774±41	1637±19
ε=0.8	1848±46	1771±42	1620±16	1853±43	1774±40	1636±18	1845±42	1762±46	1630±17
ε=0.7	1839±42	1755±41	1612±8	1840±47	1759±51	1624±23	1832±46	1749±55	1629±20

References

(1) Shah NJ, et al, *NeuroImage* 2001;14:1175–1185. (2) Deichmann R. *Magn. Reson. Med.* 2005;54:20–27. (3) Silver MS, et al, *J. Magn. Reson.* 1984;59:347–351. (4) Garwood M, et al, *J. Magn. Reson.* 1991;94:511–525. (5) Haase A. *Magn. Reson. Med. 1990*;13:77–89.

Acknowledgements

The study was supported by grants from the Ministry of Education, Culture, Sports, Science and Technology (Japan), and University of Niigata.